Ruano-Sánchez, D.; Cored-Bandrés, J.; Azenha, C.; Pérez-Dieste, V.; Mendes, A.; Mateos-Pedrero, C.; Concepción Heydorn, P. (2019). Dynamic Structure and Subsurface Oxygen Formation of a Working Copper Catalyst under Methanol Steam Reforming Conditions: An in Situ Time-Resolved Spectroscopic Study. ACS Catalysis. 9(4):2922-2930. https://doi.org/10.1021/acscatal.8b05042

"Dynamic structure and subsurface oxygen formation of a working copper catalyst under MSR conditions"
An *in situ* time resolved spectroscopic study

Daniel Ruano[a,b], Jorge Cored[b], Cátia Azenha[c], Virginia Pérez-Dieste[a], Adelio Mendes[c], Cecilia Mateos-Pedrero[c,*], Patricia Concepción[b,*]

[a] *ALBA synchrotron light source, Carrer de la Llum 2-26, 08290 Cerdanyola del Vallès, Spain*

[b] *Instituto de Tecnología Química, Universitat Politècnica de València-Consejo Superior de Investigaciones Científicas (UPV-CSIC), Avenida de los Naranjos s/n, 46022 Valencia, Spain*

[c] *LEPABE - Laboratory for Process Engineering, Environment, Biotechnology and Energy, Faculty of Engineering, University of Porto, Rua Dr. Roberto Frias, 4200-465 Porto, Portugal*

- **ABSTRACT**

The dynamic behavior of a $CuO/ZnO/Ga_2O_3$ catalyst under Methanol Steam Reforming (MSR) reaction conditions promoted by a high dispersion of the copper nanoparticles and defect sites of a non-stoichiometric $ZnGa_2O_4$ spinel phase has been observed, where structural changes taking place in the initial state of the reaction determine the final state of the catalyst in stationary reaction conditions. Mass Spectrometry (MS) studies under transient conditions coupled to X-Ray Photoelectron Spectroscopy (XPS) have shown copper oxidation to Cu^+ in the initial state of the reaction (TOS = 4 min), followed by a fast reduction of the outer shell to Cu^0, while keeping dissolved oxygen species in the inner layers of the nanoparticle. The presence of this subsurface oxygen impairs a positive charge to the uppermost surface copper species, i.e. $Cu^{\delta+}$, which undoubtedly plays an important role on the MSR catalytic activity. The detection of these features, unperceived by conventional spectroscopic and catalytic studies, has only been possible by combining synchrotron NAP-XPS studies with transient studies performed in a low volume catalytic reactor connected to MS and linked with Raman and laboratory scale XPS studies.

Keywords NAP-XPS, methanol steam reforming, copper, subsurface oxygen, *in situ* spectroscopy

- **INTRODUCTION**

Reaction induced catalyst restructuration with modification in the catalyst oxidation state, metal particle size and morphology is observed in many catalytic processes,[1-3] controlling the reaction selectivity. While these bulk modifications are easily detected using conventional spectroscopic tools, there are some catalytic features as, for instance, surface reconstruction or structural changes taken place in the very early stage of the reaction that remain undetectable unless non-conventional characterization tools are applied.[4,5] In the last years and boosted by advanced spectroscopic techniques (many of them with *in situ* possibilities), the role of the subsurface region of the catalyst in the catalytic process and reactant induced surface reconstruction has engendered great scientific interest.[6-9] For instance, carbon dissolution in subsurface sites of Pd catalysts has been thoroughly investigated using Near Ambient Pressure X-Ray Photoelectron Spectroscopy (NAP-XPS) and their role in the selective hydrogenation path of alkynes has been demonstrated.[8] In addition, the role of surface and subsurface oxygen species in the selective or unselective methanol oxidation on a Cu foil has also been reported.[9,10] It was shown that the presence of subsurface species modifies the surface electronic properties of the catalyst and, accordingly, their reactivity. Based on these studies, a critical understanding of both surface and subsurface dynamics is imperative and also very challenging, requiring support of modern spatiotemporal and surface-sensitive enhanced spectroscopies with the possibility to work under reaction conditions. In this sense, synchrotron based NAP-XPS is a very powerful characterization technique, where the high brilliance of the radiation insures high sensitivity and the wide range in the X-ray energy permits to perform analysis at different sample depth.[5,11] In addition, the use of transient studies with temporal resolution is very helpful in investigating the state of the catalyst in the very early stage of the reaction.[12] Altogether allows delineating true structural-reactivity relations, key point for a rational design of the catalyst.

Recently, a highly active and selective $CuO/ZnO/Ga_2O_3$ catalyst has been developed, two times more active than the commercial $CuO/ZnO/Al_2O_3$ catalyst from Süd Chemie in the low temperature methanol steam reforming (MSR) process.[13] Copper dispersion, related to its small particle size, around 10 nm, has been reported to be a key aspect in its catalytic performance. Besides particle size, additional parameters have also been extensively discussed in the literature for improved catalyst performance in the low temperature MSR reaction, like the role of different promoters (such as Ga_2O_3, CeO_2) in stabilizing Cu^+ species[14] (in many cases generated *in situ*), the effect of microstrain and structural disorder in the metallic Cu phase and the formation of a specific interface between copper and the metal oxide (as for instance Cu-ZnO).[15,16] Recently, some authors reported on the formation of very small and highly active copper clusters promoted by the incorporation of Ga into a Cu-Zn mixed oxide catalyst.[17] The *in*

situ adjustment of the Cu^{+}/Cu^{0} ratio has been stated and widely discussed in several works,[18,19] however few studies have been directed at evaluating structural changes of the catalyst under working conditions, specifically those taking place in the initial stage of the reaction. The aim of our work is to provide detailed insight into the structure and the dynamism of the catalyst at the molecular level and shed light into the oxidation state of copper under working conditions in the MSR reaction. To this purpose, we performed catalytic studies with temporal resolution in the early stage of the reaction using Mass Spectrometry (MS) simultaneously to Raman and XPS spectroscopic studies, and combined with time resolved NAP-XPS studies and sequential pulse experiments. Our research shows that 10 nm copper nanoparticles are susceptible to oxidation in the first 1-4 minutes of the MSR reaction, followed by a fast reduction of the copper (I) oxide shell to metallic copper, while keeping some dissolved oxygen species in inner layers of the nanoparticle. Depending on the nature of the catalyst, the degree of catalyst oxidation-reduction changes, which results in different states of the copper particle under stationary MSR conditions, influencing undoubtedly their catalytic activity. A positive role of subsurface oxygen species on the MSR catalytic activity is demonstrated.

- **EXPERIMENTAL SECTION**

Synthesis of $CuO/ZnO/Ga_2O_3$ catalysts

$CuO/ZnO/Ga_2O_3$ mixed oxides, labelled as CuZnGa and CuZnGa-OH, with the same chemical composition ($CuO/ZnO/Ga_2O_3$ = 65/25/10 wt. %, Table S1) and with properties similar to industrial catalytic formulations (high Cu loading and exposed Cu surface areas of ≥ 10 $m^2 \cdot g^{-1}$) were synthesized according to an optimized co-precipitation procedure reported previously,[13] using different precipitating agents (ammonium hydrogen carbonate for the CuZnGa sample and sodium hydroxide for the CuZnGa-OH sample. More details in SI.

Methanol steam reforming catalytic studies

MSR catalytic tests were performed at atmospheric pressure in an in-house built set-up with the following experimental conditions: steam-to-methanol molar ratio of 1.5, temperature range of 180 °C to 300 °C and a space-time ratio (W/F_{MeOH}) of 65 and 150 $kg \cdot s \cdot mol^{-1}$. Prior to the catalytic activity measurements, the catalyst was reduced *in situ* using a diluted hydrogen stream (20 vol % of H_2 balanced with N_2), at 200 °C for 1 h. More details in SI.

Near Ambient Pressure X-Ray Photoelectron Spectroscopy studies

NAP-XPS experiments were performed at the NAPP end-station of CIRCE BL24 the ALBA Synchrotron Light Source Facility. CIRCE is an undulator beamline with photon energy range 100-2000 eV. The beam spot size at the NAPP sample position is 100×30 (HxV) μm^2. The data were acquired with a Phoibos 150 NAP electron energy analyser, pass energy of 20 eV and beamline

exit slit of 20 µm. Incident photon energies of 1200 eV, 1386 eV and 1800 eV for $Cu2p_{3/2}$; 1200 eV, 1290 eV and 1800 eV for $Zn2p_{3/2}$; 1290 eV and 1386 eV for $Ga2p_{3/2}$; 1386 eV for CuLVV and 700 eV for O1s were used, allowing to probe sample depths between 2.0 nm and 5.4 nm. The probing depth was obtained using the QUASES-IMFP-TPP2M software[20] for ZnO. It calculates the inelastic mean free path using the Tanuma Powell and Penn algorithm (TPP2M).[21] The sample (80-100 mg) was pelletized and mounted onto the sample holder using a resistive button heater for sample heating. The temperature was monitored with a K-type thermocouple in direct contact with the sample. The gases were dosed into the analysis chamber using leak valves. The samples were initially treated in H_2 atmosphere during 3.5 hours at 200 °C and 3 mbar in order to reduce them. MeOH (Methanol, Reag. Ph. Eur, Panreac, purity ≥ 99.8%) and H_2O (LC-MS Ultra CHROMASOLV®, Fluka - Sigma Aldrich) were fed into the analysis chamber maintaining a constant pressure of 1.0 mbar MeOH and 1.5 mbar H_2O with the sample at 180 °C during 4 h. In the time resolved experiments, 1.0 mbar MeOH was first fed into the chamber at a temperature of 180 °C followed by 1.5 mbar H_2O dosing. Immediately after H_2O dosing, the O1s core level was collected in a sequential mode with an acquisition time of each scan of 1.6 min and at an X-ray excitation energy of 700 eV. Controlled blank experiments using a quadrupole gas analyser located at the second pumping stage of the XPS analyser shown that the water pressure in the analysis chamber is stable when starting the O1s spectra acquisition. Due to attenuation of the XPS signal during the sequential acquisition mode, the subtracted O1s XPS spectra displayed in Figure 1 were calculated relative to two different spectra (O1s at time 0.0 and O1s at time 3.2 min). The energy scales of the XPS spectra were calibrated using the Fermi edge position. The NAP-XPS data were analyzed using the CASA XPS software. Reaction products were analyzed using a Microvision-IP quadrupole residual gas analyzer from MKS Instruments, located at the second pumping stage. The m/z values used in the identification of each product were: 31 for MeOH; 2 for H_2; 18 and 17 for H_2O; 44 for CO_2 and 28 for CO.

Laboratory scale XPS studies

X-Ray photoelectron spectra of the catalysts were recorded with a SPECS spectrometer equipped with a Phoibos 150 MCD-9 multichannel analyzer, using a non-monochromatic AlKα (1486.6 eV) X-Ray source. The spectra were recorded with an X-Ray power of 50 mW, pass energy of 30 eV and under an operating pressure of 10^{-9} mbar. The sample (~10 mg) was pressed into a pellet and loaded onto the SPECS stainless steel sample holder. Before XPS analysis, the sample was submitted to different treatments in a high-pressure reactor (HPCR) directly connected under UHV to the XPS analyze chamber. XPS analysis were performed following the subsequent *in situ* treatments: i) H_2 reduction (10 mL·min^{-1} flow) at 200 °C and at atmospheric

pressure for 3 h; ii) MSR reaction at 180 °C, atmospheric pressure, in a MeOH:H_2O (1:1.5 molar ratio) reaction feed (54 mL·min^{-1} total flow) and stopping the reaction at different times; iii) H_2O flow (17 mL·min^{-1} total flow of 0.006 mol % H_2O/Ar) at 180°C for 30 min and iv) MeOH flow (17 mL·min^{-1} total flow of 0.023 mol % MeOH/Ar) at 180 °C for 15 min. In the case of methanol and water, argon was flown through two separated saturators. The XPS spectra were referenced to C1s peak (284.5 eV) and spectra treatment was performed using the CASA XPS software. Reaction products in point ii) were analysed by Gas Chromatography (GC) using Bruker 450 GC equipped with a TCD, a Mol Sieve 5A column and Ar as carrier gas.

MSR Catalytic-Mass Spectrometry studies

A home-made low volume micro-reactor (~0.15 cm^3) was used connected on line to a Balzers Mass spectrometer. The samples (~40-45 mg) were reduced in a H_2 flow (10 mL·min^{-1}) at 200 °C for 3 h, followed by purging in an Ar flow for 20 min (10 mL·min^{-1}) at 200 °C and subsequent cooling down to 180 °C under Ar flow for another 30 min. During the cooling down time, the MSR reaction feed was homogenized in a by-pass line. A MeOH and H_2O feed of 1:1.5 molar ratio was used by flowing Ar through two separated saturators. The reactor effluent was continuously monitored by MS, allowing detection of reaction product immediately after feeding MeOH + H_2O through the catalyst. Mass fragmentation (m/z) of 31 for MeOH; 2 for H_2; 18 and 17 for H_2O; 44 for CO_2 and 28 for CO were used. Blank experiments were performed in the absence of catalyst.

Pulse experiments by alternating water and methanol cycles followed by MS

The water and methanol pulse experiments were performed in the same home-made low dead volume micro-reactor as indicated above connected on line to a Balzers Mass Spectrometer. Reaction conditions were the same as in the XPS studies (point iii and iv of the laboratory scale XPS experimental section). Hence, the sample after H_2 reduction was submitted to alternating MeOH/H_2O cycles of 0.006 mol % H_2O/Ar (17 mL·min^{-1} flow) for 30 min and 0.023 mol % MeOH/Ar (17 mL·min^{-1} flow) for 15 min respectively at 180 °C, and the reaction products were followed by on line MS. After each pulse, the sample was exposed to an Ar flow (17 mL·min^{-1}) for 20 min.

Infrared studies

Infrared (IR) spectra were recorded with a Nexus 8700 FTIR spectrometer using a DTGS detector and acquiring at 4 cm^{-1} resolution. An IR cell allowing *in situ* treatments in controlled atmospheres and temperatures from -176 °C to 500 °C was connected to a vacuum system with gas dosing facility. For IR studies, the samples were pressed into self-supported wafers and

submitted to different reaction conditions. For the reduction studies, the sample was treated at 200 °C in H_2 flow (10 mL·min^{-1}) for 3 h followed by evacuation at 10^{-4} mbar at the same temperature for 1 h and cooling down to -60 °C under dynamic vacuum conditions. CO was dosed at -60 °C and at increasing pressure (0.4-8.5 mbar). IR spectra were recorded after each dosage. For the MSR studies the sample was initially reduced at 200 °C in H_2 flow (10 mL·min^{-1}) for 3 h, cooling down in H_2 flow to 180 °C and submitted to a MeOH:H_2O feed of 1:1.5 at 180 °C for 1 h. Afterwards, the sample was evacuated at 10^{-4} mbar and cooling down to -60 °C under dynamic vacuum conditions. CO was dosed at -60 °C and at increasing pressure (0.4-8.5 mbar). IR spectra were recorded after each dosage. Methanol and water were fed by flowing Ar through two separated saturators.

Raman studies

Raman spectra were recorded using a 514 nm-excitation laser on a Renishaw Raman spectrometer ("Reflex") equipped with a CCD detector. The laser power on the samples was 25 mW and a total of 5 acquisition were taken for each spectra. For the *in situ* studies, a Linkam CCR1000 catalytic system was used. The sample was initially reduced in a H_2 flow (10 mL·min^{-1}) at 200 °C for 3 h followed by cooling down to 180 °C in Ar and submitted to H_2O flow 10 mL·min^{-1} (0.006 mol % H_2O/Ar) for around 2 h. Spectra were acquired at specific reaction times. After water exposure, the gas was switched to a methanol flow (17 mL·min^{-1}) at 0.023 mol % MeOH/Ar and Raman spectrum was collected immediately.

▪ RESULTS AND DISCUSSION

Two catalysts with identical chemical composition ($CuO/ZnO/Ga_2O_3$, 65/25/10 wt. %), but prepared using different precipitating agents i.e. ammonium hydrogen carbonate and sodium hydroxide at a fixed pH were studied, labeled as CuZnGa and CuZnGa-OH respectively (SI for details). The Cu particle size obtained from XRD analysis is 10 nm in the CuZnGa sample and 35 nm in the CuZnGa-OH sample. Moreover, the formation of a cubic $ZnGa_2O_4$ spinel phase can be identified in the CuZnGa sample by XRD analysis, being not present in the CuZnGa-OH sample (Figure S1). The MSR activity and selectivity at different space time ratios (i.e., m_{cat}/F_{MeOH}) is given in Table S1 and reported recently.[13] Clearly, a higher activity and MSR selectivity are shown in CuZnGa catalyst, specifically in the low temperature range, i.e. 180 °C.[13] At this temperature and a space time ratio of 150 kg·s·mol^{-1}, a 80.0% methanol conversion with 99.5% selectivity to CO_2 is obtained, a value notably higher than that obtained by the CuZnGa-OH catalyst (57.9% methanol conversion) and by other catalysts reported in the literature or even in the commercial $CuO/ZnO/Al_2O_3$ catalyst from Süd-Chemie (labeled as G66-MR) (55.4% methanol conversion) catalysts. The selectivity to CO remains in all catalysts below 0.5 mol % at 180 °C. Encouraged by

the high catalytic activity displayed by the CuZnGa sample, a deeper insight into the nature of active sites was obtained by combining several spectroscopies focusing on the dynamics of the catalyst under reaction conditions.

NAP-XPS studies. The state of the catalysts under H_2 reduction (2.5 mbar) at 200 °C and under MSR reaction conditions at 180 °C and in 1.0 mbar MeOH and 1.5 mbar H_2O was followed by *in situ* photoelectron spectroscopy using synchrotron radiation. Despite of the lower working pressure, the reaction product analysis using a quadrupole residual gas analyzer installed in the second pumping stage of the NAP-XPS analyzer, shows similar kinetics regarding CO_2/CO ratio and CO_2 formation rate as it does in the MSR catalytic studies performed at 1 bar (Tables S1 and S2), confirming that the NAP-XPS results provide reliable correlation between the electronic structure of the catalyst surface and its catalytic performance.

Table 1. Binding energies of $Zn2p_{3/2}$, $Ga2p_{3/2}$ and $Cu2p_{3/2}$ core levels at different sample depths of the CuZnGa sample in H_2 (2.5 mbar) and MSR conditions (1.0 mbar MeOH and 1.5 mbar H_2O, total pressure 2.5 mbar) at stationary conditions of 3 h.

Element Energy level	hv (eV)[a]	Sampling depth (nm)[b]	BE (eV) (H_2)	BE (eV) (MSR)	ΔBE (eV) (MSR-H_2)
$Zn2p_{3/2}$	1200	2.0	1021.96	1022.30	+0.34
	1290	2.5	1022.17	1022.30	+0.13
	1800	5.0	-	1022.11	-
$Ga2p_{3/2}$	1290	2.0	1118.30	1118.57	+0.27
	1386	2.5	1118.30	1118.50	+0.20
$Cu2p_{3/2}$	1200	2.5	932.58	932.58	0.00
	1386	3.4	932.35	932.70	+0.35
	1800	5.4	932.35	932.30	0.00

[a]X-Ray Excitation Energy. [b]Sampling depth was calculated using the QUASES-IMFP-TPP2M software for ZnO.

The binding energies (BE) of the $Zn2p_{3/2}$, $Ga2p_{3/2}$ and $Cu2p_{3/2}$ NAP-XPS core levels acquired at different sample depths and in presence of different reactants are given in Table 1 for the CuZnGa sample and their spectra shown in the Supporting Information (Figure S2). The BE of the $Zn2p_{3/2}$ and $Ga2p_{3/2}$ core levels corresponds to an oxidation state of Zn^{2+} and Ga^{3+} respectively.[22,23] In the case of Cu, both the $Cu2p_{3/2}$ BE and the Cu LVV AES peak (at 918.5 eV)

correspond to Cu^0.[10] Slight BE shifts can be observed for the different elements depending on the probed sample depth and the gas environment. Thus, in the H_2 reduced sample, the BE of $Zn2p_{3/2}$ in the upper layer is slightly lower, what could be due to adjacent surface defects; while in case of $Cu2p_{3/2}$ the BE in the upper layer is barely higher due to a slight positive charge of the copper surface. Under MSR conditions, both $Zn2p_{3/2}$ and $Ga2p_{3/2}$ core levels at 2.0 and 2.5 nm probing depths shift to higher BE (ΔBE = +0.34 eV and +0.13 eV respectively for $Zn2p_{3/2}$) and (ΔBE = +0.27 eV and +0.20 eV respectively for $Ga2p_{3/2}$), which can be ascribed to surface re-oxidation, i.e., depletion of surface defects generated during H_2 reduction. In both cases, this effect is more pronounced in the upper surface layers. This re-oxidation is probably related to H_2O activation, which may take place on defective sites of the Zn-Ga oxide layer. On the other hand, regarding the nature of copper species under MSR conditions, the most remarkable observation is the +0.35 eV shift experienced in the $Cu2p_{3/2}$ core level at a probing depth of 3.4 nm, not observed when acquiring at a lower sampling depth of 2.5 nm or at a higher depth of 5.4 nm. The presence of subsurface oxygen may account for this peculiar behavior, shifting the corresponding $Cu2p_{3/2}$ BE to slightly higher values. This result lead us to propose a core-shell structure of the copper particle under MSR conditions as depicted in Scheme 1, where the outer shell (1) is metallic, the intermediate shell (2) slightly oxidized and the inner core (3) metallic.

Scheme 1. Proposed core-shell structure of the CuZnGa sample under steady state MSR conditions underlining the presence of subsurface oxygen species in the copper nanoparticle.

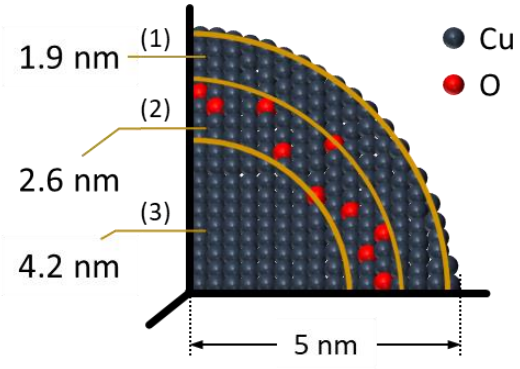

In order to follow how catalyst re-oxidation takes place by H_2O activation, the O1s core level was acquired under time resolved conditions, every 1.6 min, using a 700 eV X-Ray energy. Interestingly, at the first scan immediately after H_2O dosing (Figure 1a,c), a new peak at 530.4 eV can be discerned, which may correspond to oxygen species associated with oxidized copper (Cu_2O).[10,24,25] This feature disappears in the following two scans (not shown) and a broad component with two maxima at ~531.1 eV and ~532.5 eV starts to appear (Figure 1b,d), which may correspond to new oxygen species associated with re-oxidation of the Zn-Ga oxide phase

and/or hydroxyl groups.[26,27] Assignation of the aforementioned O1s components to oxygenated hydrocarbons like, for instance, methoxy/acetate (532.0 eV) or formate groups (531.4 eV)[10,24,25,28-30] can be excluded in our case, since no new C1s XPS signal is detected at the experimental conditions.

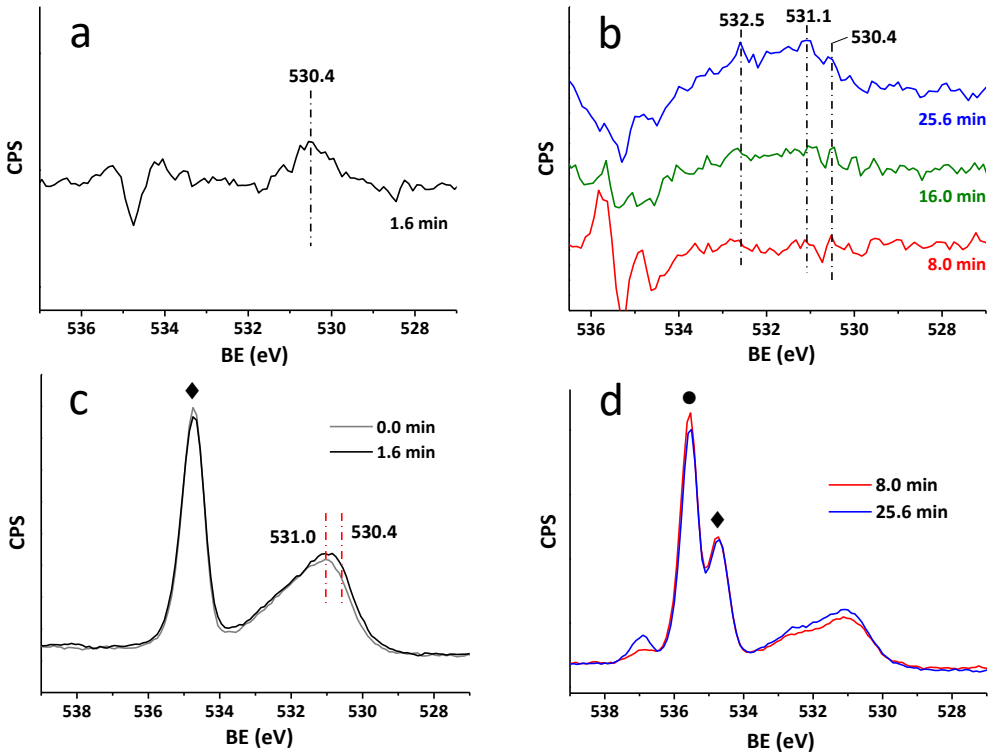

Figure 1. Evolution of the O1s core level XPS spectra acquired at 700 eV X-Ray excitation energy after co-addition of 1.5 mbar H_2O at 180 °C on the CuZnGa sample which was exposed to 1.0 mbar MeOH. Spectra were acquired at 1.6 min time interval. "a" and "b": subtracted spectra relative to t = 0.0 ("a") and t = 3.2 min ("b") (details in SI). "c" and "d": O1s original spectra. Spectra "a" and "c" correspond to the first scan immediately after H_2O dosing. Spectra "b" and "d" correspond to scans at different times. Total acquisition time: 26 min. ● and ♦ correspond to the O1s peak of gas phase H_2O (535.5 eV) and MeOH (534.7 eV) respectively.

Meaningfully, the above observed shift in the $Cu2p_{3/2}$ core level of the intermediate shell of the copper nanoparticle is not observed in the other samples analyzed under similar NAP-XPS-MSR conditions, like the CuZnGa-OH and the commercial G66-MR sample (Tables S3 and S4), which are less active and selective in the low temperature-MSR reaction. Being aware that many factors influence the catalytic performance of the catalysts in the MSR reaction, the presence of these subsurface oxygen species could modify the electronic properties of the metallic copper surface or generate new defect surface sites, where methanol and water activation and thus CO_2 formation could be favored.[9] Indeed, this was confirmed by IR studies of CO titration

performed on the CuZnGa sample, where electronic modification of the surface copper atoms conferring them a positive charge was detected after being exposed to *in situ* MSR conditions. As depicted in Figure 2, the initial IR band at 2095 cm^{-1}, corresponding to CO interacting with metallic copper sites (Cu^0)[31] in the *in situ* H_2 reduced CuZnGa sample, is not present after MSR while a new broad band at higher frequency (2110 cm^{-1}) is detected. This high frequency IR band can be associated with CO interacting with positively charged metal species[32,33] i.e., $Cu^{\delta+}$. In contrast, reduced Cu^0 is observed on the CuZnGa-OH sample after *in situ* MSR conditions (Figure S3).

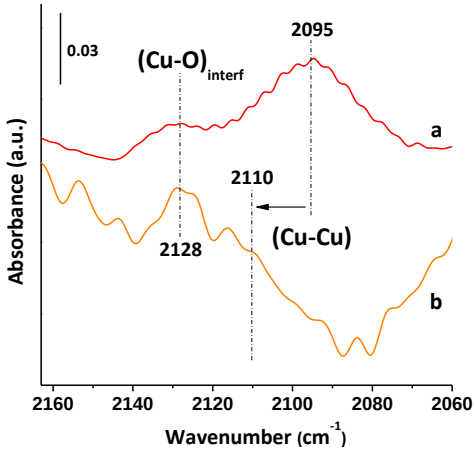

Figure 2. IR spectra of CO adsorption at -60 °C on the CuZnGa sample: a) *In situ* H_2 reduced sample; b) Sample after 1 h MSR. The IR band at 2128 cm^{-1} corresponds to copper – (Zn-Ga) metal oxide interface sites $(Cu\text{-}O)_{interf}$.

Since this subsurface oxygen and electronic perturbation of surface atoms are only observed on the most active catalyst (CuZnGa), we can infer on a positive effect improving the MSR performance. The oxidation state of the active copper species in MSR has been widely discussed in the literature, where some authors proposed Cu^+ as active site,[14,16,18,19] enhancing, in that way, methanol activation. But, to our knowledge, no evidence and no discussion of subsurface oxygen species resulting in $Cu^{\delta+}$ surface sites has been reported in the MSR reaction working on copper based catalysts. This $Cu^{\delta+}$, similar to the literature discussed Cu^+, may act positively on the catalytic performance.

The formation of this subsurface oxygen species (only detected in the CuZnGa sample) implies a dynamic evolution of the catalyst under MSR conditions, which is barely detected by NAP-XPS studies. In order to deepen into this dynamic behavior, catalytic studies with temporal resolution in the early stages of the reaction monitored by MS analysis and combined with laboratory scale XPS spectroscopic studies were performed.

Catalytic–Mass Spectrometry studies. Following the product evolution of the MSR reaction of the CuZnGa sample by MS-using a low volume micro-reactor, a sharp increase in the H_2 signal (m/z = 2) in the initial state of the reaction is observed (Figure 3). It achieves a maximum value at ~4 min time on stream (TOS), and then starts to decline until reaching a stationary value at ~12 min TOS. Notoriously, the initial H_2 formation shows a small shoulder at 1 min TOS. Analyzing the evolution of the CO (m/z = 28) and CO_2 (m/z = 44), a concomitant sharp increase in the CO signal can be observed in the first one minute of reaction with practically no CO_2 formation. At 4 min TOS, the H_2 signal achieves its maximum value while no appreciable changes in the other signals can be observed, and at 12 min TOS, all products achieve constant values. Diffusional effects in the catalytic cell as responsible of the sharp increase in H_2 can be neglected since methanol (m/z = 31) and water (m/z = 17) are stabilized in a timeframe below one minute. Moreover, a blank experiment without catalyst or in the presence of unreduced (i.e. calcined) catalyst shows no evolution of H_2. The first H_2 and CO formation at a timeframe of 1 min may come from the methanol decomposition (MD) reaction, while the subsequent sharp increase of H_2 (in absence of other mass fragments) may be ascribed to catalyst oxidation. The short timeframe during which the initial H_2 release occurs prevent its detection in a conventional reactor setup.

Catalyst surface re-oxidation of the defective Zn-Ga oxide surface layer under MSR conditions was already observed in the NAP-XPS studies. While some evidences of copper oxidation were also obtained from those studies, more solid insight was needed in order to confirm it. Therefore, laboratory based XPS studies, where the reaction takes place at atmospheric pressure in a high-pressure reactor (HPCR) directly connected (under UHV) to the XPS analysis chamber, were performed. In order to ensure similar catalytic behavior, the reaction products were followed by GC.

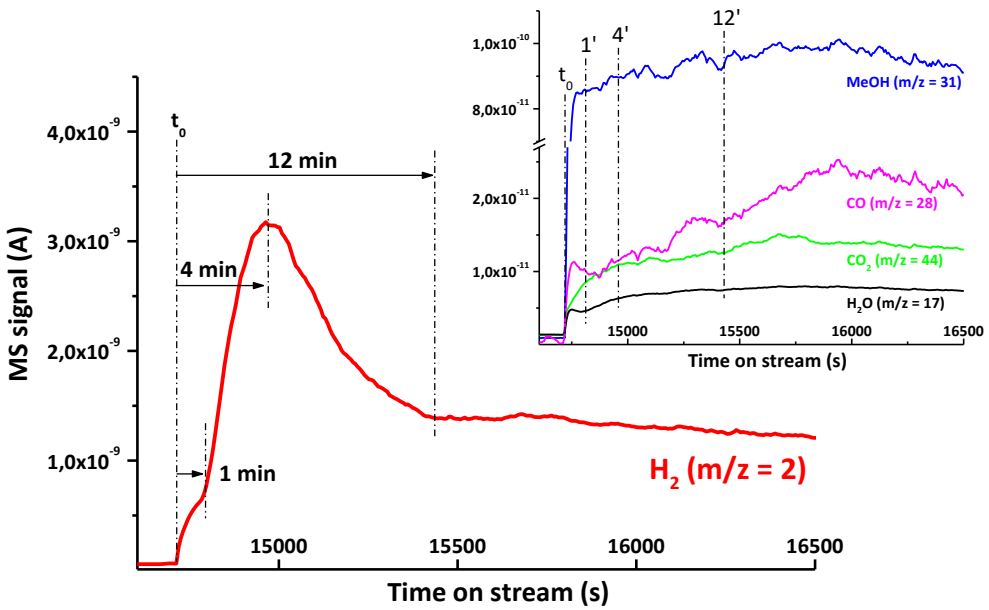

Figure 3. H_2 release during the MSR reaction performed at 180 °C on the CuZnGa sample monitored by Mass Spectrometry. Inset shows the evolution of the rest of products.

Laboratory scale XPS studies. The MSR reaction in HPCR was stopped at 4 min (when H_2 GC signal achieved its maximum value) and at 120 min (when the H_2 reached a stationary value). In both situations, the sample was transferred under high vacuum to the XPS chamber for analysis. Stopping the reaction at 4 min, the Cu LVV spectrum shows, in addition to the main peak at 918.4 eV due to Cu^0, a component at 916.2 eV due to Cu^+, which disappears after 120 min of reaction (Figure 4). Based on this result, the initial H_2 release can be ascribed to the partial oxidation of the copper particle, besides Zn-Ga surface re-oxidation. The initial oxidized copper species are then reduced during the course of the reaction. Probably, only the shell of the copper particle is reduced under reaction conditions, keeping the core slightly oxidized and explaining, in that way, the presence of subsurface species detected under stationary reaction conditions in the NAP-XPS studies.

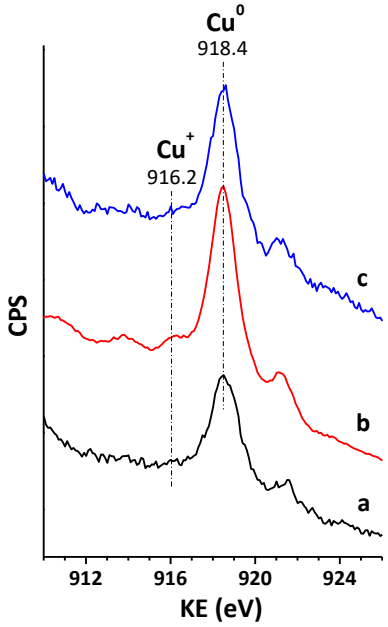

Figure 4. CuLVV AES spectra showing the evolution of Cu species in the CuZnGa sample: a) *In situ* H_2 reduced sample; and b) and c) under MSR reaction conditions stopping at 4 min and 120 min respectively. Catalytic reaction was performed in a HPCR connected under UHV to the XPS analyse chamber.

Pulse experiments followed by XPS and MS. In order to understand in more detail the redox behavior of the copper species and how it influences the final state of the catalyst, pulse experiments were performed by alternating cycles of methanol (0.023 mol % MeOH/Ar) and water (0.006 mol % H_2O/Ar), followed by on line MS. Additionally, the state of the catalysts under similar pulse experiments was monitored by laboratory scale XPS.

Based on XPS data, the initial reduced copper species of the pre-reduced CuZnGa sample are oxidized to Cu^+ in the presence of H_2O ($Cu2p_{3/2}$ BE of 933.0 eV and Cu(α), (α = auger parameter) of 1849.1 eV), while reduced in the presence of methanol ($Cu2p_{3/2}$ BE of 932.7 eV and Cu(α) of 1851.2 eV). This behavior is shown to be independent of whether the pre-reduced catalyst is first exposed to H_2O (Cycle 1, table 2) or to MeOH (Cycle 2, table 2). Moreover, surface segregation of Cu in the presence of H_2O, and of Zn and Ga in the presence of methanol is observed based on the chemical analysis of surface elements, where the Cu/Zn molar ratio changes from ~2.5 (in H_2O) to ~1 (in MeOH), and the Cu/Ga molar ratio from ~12 (in H_2O) to ~5 (in MeOH). This behavior is reversible along several cycles, revealing a high dynamism of the catalysts depending on the reactant conditions.

Table 2. Electron binding energies extracted from the XPS data of the CuZnGa sample exposed to sequential H_2O/MeOH cycles.

CuZnGa: CYCLE 1

Gas	$Cu2p_{3/2}$ BE (eV)	Cu(α)[a] (eV)	Cu/Zn	Cu/Ga	Zn/Ga
H_2	932.7	1851.3	1.0	5.5	5.5
H_2O	933.0	1849.1	1.3	8.5	6.4
MeOH	932.8	1851.3	0.9	5.3	5.6
H_2O	933.0	1849.0	1.7	9.7	5.7

CuZnGa: CYCLE 2

Gas	$Cu2p_{3/2}$ BE (eV)	Cu(α)[a] (eV)	Cu/Zn	Cu/Ga	Zn/Ga
H_2	932.7	1851.3	1.0	5.5	5.5
MeOH	932.7	1851.3	0.8	4.9	5.8
H_2O	933.0	1849.1	2.6	14.4	5.5
MeOH	932.7	1851.2	0.8	4.8	5.5
H_2O	933.0	1849.0	2.3	12.7	5.5

[a]Cu auger parameter (α = $Cu2p_{3/2}$ (BE) + CuLVV (KE)). KE = Kinetic Energy.

Interestingly, reproducing the same pulses in a micro-reactor connected to MS, an initial high H_2 release can be observed in the first pulse of H_2O, while it markedly decreases after having pulsed methanol on the sample (Figure 5). Assuming that H_2 comes from catalyst oxidation, this behavior can be explained by an initial fast oxidation of the reduced copper particle, which is reduced in the subsequent methanol pulse. If methanol only reduces the outer particle layers (i.e., particle shell), one can assess that the H_2 release in the second H_2O pulse (due to shell re-oxidation) should be lower, as effectively is the case, and the subsequent "oxo-reduction" cycles would take place on the more exposed surface layers of the copper particle (see insets of Figure 5). This confirms our previous result, where *in situ* generated subsurface oxygen species come from an initial fast oxidation of the copper particle, followed by surface reduction, while the core remains slightly oxidized under MSR conditions.

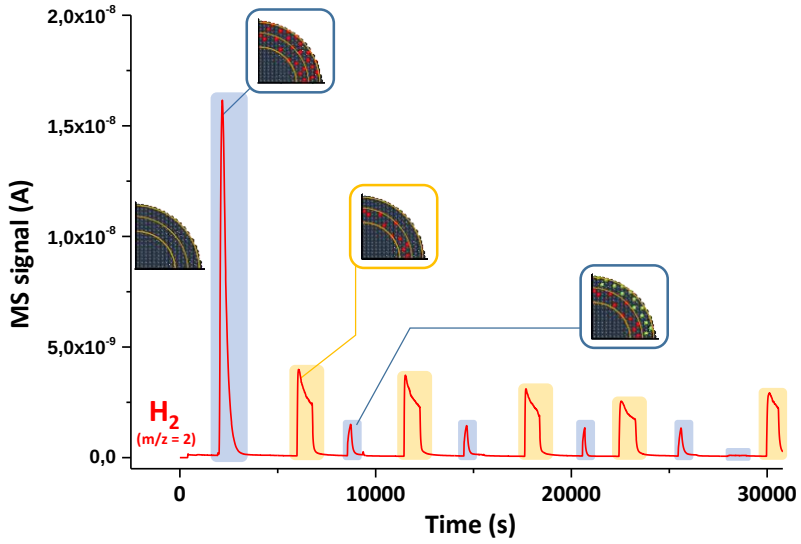

Figure 5. Mass spectrum monitoring the H_2 release during sequential H_2O (blue) and MeOH (yellow) cycles at 180 °C in the CuZnGa sample. After each pulse, the sample was exposed to Ar flow for 20 min. Red and green spheres correspond to oxygen atoms.

This redox behavior of the copper species is only observed in the CuZnGa sample. In the case of the CuZnGa-OH sample, the copper remains in a reduced state during MSR reaction, as deduced from NAP-XPS studies and laboratory XPS studies, where the reaction is stopped at specific reaction times (Figure S4-S5 and Table S5). While an initial H_2 release can also be observed in the time resolved catalytic–MS studies, it has to be related to re-oxidation of the catalyst surface Zn–Ga oxide layer, as observed in the NAP-XPS study. Moreover, the extent of catalyst oxidation-reduction and surface segregation of the different elements in the sequential cycles of water and methanol is less pronounced than in the CuZnGa sample, which would explain the less dynamic behavior of the CuZnGa-OH sample (Table S6).

On the other hand, water activation is a key factor in the promotion of MSR process, as evidenced from *in situ* Raman studies.

Raman studies. Figure 6a shows new Raman bands at 212, 184 and 148 cm^{-1} formed in the presence of water after a time on stream of 24 min in the CuZnGa sample, while similar bands are formed in the CuZnGa-OH sample after 41 min (Figure 6b). These bands can be ascribed to OH groups,[34] where the formation of surface "oxo" species (by surface re-oxidation) cannot be completely discarded. The different time response observed on both samples can be used as indication of their different reactivity toward dissociation of water. All these bands disappear immediately by switching the gas feed to methanol, indicating their high reactivity (Figure S6).

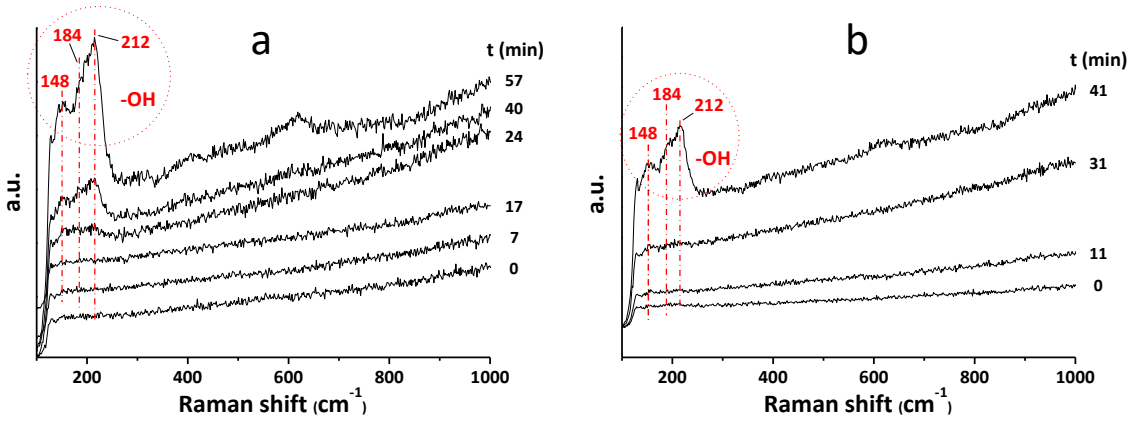

Figure 6. Raman spectra of the CuZnGa sample (Figure 6a) and of the CuZnGa-OH sample (Figure 6b) exposed to a 0.006 mol % H_2O/Ar flow (10 mL·min^{-1}) at 180 °C. Spectra were acquired at specific reaction times.

These Raman results are not fully unexpected taking into consideration the bigger size of the copper particle and the less amount of surface defect sites in the CuZnGa-OH sample than in the CuZnGa sample, resulting in a lower ability toward water activation and lower affinity of the copper particle to be oxidized by water, maintaining in a metallic state under MSR reaction.

- **CONCLUSIONS**

In this work, by the application of temporal resolution catalytic studies and synchrotron NAP-XPS, a dynamic behavior of the CuZnGa catalyst could be found, where surface copper atoms remain in a metallic state, while they are electronically perturbed by the presence of subsurface oxygen species. This undoubtedly influences the catalytic behavior of the system in the MSR reaction, enhancing its performance. The presence of these subsurface oxygen species is due to a fast oxidation and further reduction of the copper particle, events which take place in the initial stage of the reaction, and results undetected using a conventional reaction setup. This behavior, observed on the CuZnGa sample, seems to be promoted by a high copper dispersion and the presence of defect surface sites on which water can be easily activated, while it has not been observed on catalysts with the same chemical composition but featuring larger particle size and a less defective surface layer. Finally, it is important to highlight how the synthesis conditions and the history of the catalysts affect their final state, and therefore, their catalytic behavior, which requires the use of spatiotemporal resolved spectroscopies with *in situ* capabilities.

▪ ASSOCIATED CONTENT

Supporting information includes detailed experimental section; sample characterization; catalytic data of the CuZnGa, CuZnGa-OH and commercial samples in the MSR reaction; NAP-XPS on line Mass Spectrometry analysis; $Zn2p_{3/2}$, $Ga2p_{3/2}$ and $Cu2p_{3/2}$ NAP-XPS core levels of the CuZnGa sample under H_2 and MeOH/H_2O atmospheres; NAP-XPS data of the CuZnGa-OH and G66-MR commercial sample; IR spectra of CO adsorption on the CuZnGa-OH and CuZnGa samples after *in situ* MSR; catalytic-Mass Spectrometry studies performed on the CuZnGa-OH sample and laboratory scale XPS studies on the CuZnGa-OH sample after MSR stopping at 4 min and 120 min; pulse experiments by alternating MeOH and H_2O cycles on the CuZnGa-OH sample followed by XPS; Raman studies of methanol flow on a water pre-activated CuZnGa sample.

▪ AUTHOR INFORMATION

Corresponding authors

*pconcepc@upvnet.upv.es

*cmpedrero@yahoo.es

ORCID

Patricia Concepción 0000-0003-2058-3103

Cecilia Mateos-Pedrero 0000-0002-8836-089X

Author contributions

All authors contributed equally

Notes

The authors declare no competing financial interest

▪ ACKNOWLEDGMENTS

The research leading to these results has received funding from the European Union's Seventh Framework Programme (FP/2007-2013) for the Fuel Cells and Hydrogen Joint Technology Initiative under grant agreement nº [303476]. Part of this work was financially supported by the following projects: (i) Project POCI-01-0145-FEDER-006939 (Laboratory for Process Engineering, Environment, Biotechnology and Energy – UID/EQU/00511/2013) funded by the European Regional Development Fund (ERDF), through COMPETE2020 - Programa Operacional Competitividade e Internacionalização (POCI) and by national funds, through FCT - Fundação para a Ciência e a Tecnologia; (ii) NORTE-01-0145-FEDER-000005 – LEPABE-2-ECO-INNOVATION, supported by North Portugal Regional Operational Programme (NORTE 2020), under the Portugal 2020 Partnership Agreement, through the European Regional Development Fund (ERDF) and (iii) the Spanish Government-MINECO through "Severo Ochoa" Excellence Programme (SEV-2016-0683). D. R. thanks European Research Council project SYNCATMATCH

(671093). J. C. thanks the Spanish Government (MINECO) for a “Severo Ochoa” grant (BES-2015-075748). The NAP-XPS experiments were performed at the NAPP branch of the CIRCE beamline at the ALBA Synchrotron with the collaboration of ALBA staff.

- **REFERENCES**

(1) Liu, L.; Zakharov, D. N.; Arenal, R.; Concepción, P.; Stach, E. A.; Corma, A. Evolution and Stabilization of Subnanometric Metal Species in Confined Space by In Situ TEM. *Nat. Commun.* **2018**, *9*, 574 DOI: 10.1038/s41467-018-03012-6.

(2) Concepción, P.; Garcia, S.; Hernandez-Garrido, J. C.; Calvino, J. J.; Corma, A. A Promoting Effect of Dilution of Pd Sites Due To Gold Surface Segregation Under Reaction Conditions on Supported Pd–Au Catalysts for the Selective Hydrogenation of 1,5-Cyclooctadiene. *Catal. Today*. **2016**, *259*, 213-221.

(3) Moliner, M.; Gabay, J. E.; Kliewer, C. E.; Carr, R. T.; Guzman, J., Casty, C. L.; Serna, P.; Corma, A. Reversible Transformation of Pt Nanoparticles into Single Atoms inside High-Silica Chabazite Zeolite. *J. Am. Chem. Soc*. **2016**, *138*, 15743-15750.

(4) Divins, N. J.; Angurell, I.; Escudero, C.; Perez-Dieste, V.; Llorca, J. Influence of the Support on Surface Rearrangements of Bimetallic Nanoparticles in Real Catalyst. *Science* **2014**, *346*, 620-623.

(5) Escudero, C.; Salmeron, M. From Solid–Vacuum to Solid–Gas and Solid–Liquid Interfaces: In Situ Studies of Structure and Dynamics under Relevant Conditions. *Surf. Sci.* **2013**, *607*, 2-9.

(6) Bluhm, R.; Hävecher, M.; Zafeiratos, S.; Teschner, D.; Vass, E.; Schnörch, P.; Knop-Gericke, A.; Schlögl, R.; Lizzit, S.; Dubin, P.; Barinov, A.; Kiskinova, M. Monitoring In Situ Catalytically Active States of Ru Catalysts for Different Methanol Oxidation Pathways. *Phys. Chem. Chem. Phys.* **2007**, *9*, 3648-3657.

(7) Lee, A. F.; Ellis, C. V.; Naughton, J. N.; Newton, M. A.; Parlett, C. M. A.; Wilson, K. Reaction-Driven Surface Restructuring and Selectivity Control in Allylic Alcohol Catalytic Aerobic Oxidation Over Pd. *J. Am. Chem. Soc*. **2011**, *133*, 5724-5727.

(8) Teschner, D.; Borsodi, J.; Wootsch, A.; Revay, Z.; Hävecker, M.; Knop-Gericke, A.; Jackson, D.; Schlögl, R. The Roles of Subsurface Carbon and Hydrogen in Palladium-Catalyzed Alkyne Hydrogenation. *Science* **2008**, *320*, 86-89.

(9) Bluhm, H.; Hävecker, M.; Knop-Gericke, A.; Kleimenov, E.; Schlögl, R. Methanol Oxidation on a Copper Catalyst Investigated Using in Situ X-ray Photoelectron Spectroscopy. *J. Phys. Chem. B.* **2004**, *108*, 14340-14347.

(10) Bukhtiyarov, V. I.; Prosvirin, I. P.; Tikhomirov, E. P.; Kaichev, V. V.; Sorokin, A. M.; Evstigneev, V. V. In Situ Study of Selective Oxidation of Methanol to Formaldehyde over Copper. *React. Kinet. Catal. Lett.* **2003**, *79*, 181-188.

(11) Salmeron, M.; Schlögl, R. Ambient Pressure Photoelectron Spectroscopy: A New Tool for Surface Science and Nanotechnology. *Surf. Sci. Rep.* **2008**, *63*, 169-199.

(12) Moussa, S.; Concepcion, P.; Arribas, M. A.; Martinez, A. Nature of Active Nickel Sites and Initiation Mechanism for Ethylene Oligomerization on Heterogeneous Ni-beta Catalysts. *ACS Catal.* **2018**, *8*, 3903-3912.

(13) Ribeirinha, P.; Mateos-Pedrero, C.; Boaventura, M.; Sousa, J.; Mendes, A. $CuO/ZnO/Ga_2O_3$ Catalyst for Low Temperature MSR Reaction: Synthesis, Characterization and Kinetic Model. *Appl. Catal. B.* **2018**, *221*, 371-379.

(14) Oguchi, H.; Kanai, H.; Utani, K.; Matsumura, Y.; Imamura, S. Cu_2O as Active Species in the Steam Reforming of Methanol by CuO/ZrO_2 Catalysts. *Appl. Catal.* **2005**, *293*, 64-70.

(15) Kniep, B. L.; Girgsdies, F.; Ressler, T. Effect of Precipitate Aging on the Microstructural Characteristics of Cu/ZnO Catalysts for Methanol Steam Reforming. *J. Catal.* **2005**, *236*, 34-44.

(16) Sá, S.; Silva, H.; Brandão, L.; Sousa, J.; Mendes, A. Catalysts for Methanol Steam Reforming - A Review. *Appl. Catal. B.* **2010**, *99*, 43-57.

(17) Tong, W.; West, A.; Cheung, K.; Yu, K. M.; Tsang, S. C. E. Dramatic Effects of Gallium Promotion on Methanol Steam Reforming Cu–ZnO Catalyst for Hydrogen Production: Formation of 5 Å Copper Clusters from $Cu–ZnGaO_x$. *ACS Catal.* **2013**, *3*, 1231-1244.

(18) Mrad, M.; Gennequin, C.; Aboukais, A.; Abi-aad, E. Cu/Zn-Based Catalysts for H_2 Production Via Steam Reforming of Methanol. *Catal. Today* **2011**, *176*, 88-92.

(19) Das, D.; Llorca, J.; Dominguez, M.; Colussi, S.; Trovarelli, A.; Gayen, A. Methanol Steam Reforming Behavior of Copper Impregnated over $CeO_2–ZrO_2$ Derived from a Surfactant Assisted Coprecipitation Route. *Int. J. Hydrogen Energy* **2015**, *40*, 10463-10479.

(20) Tougaard, S. QUASES: Software packages to characterize surface nano-structures by analysis of electron spectra. http://www.quases.com/products/quases-imfp-tpp2m/

(21) Tanuma, S.; Powell, C. J.; Penn, D. R. Calculations of Electron Inelastic Mean Free Paths. V. Data for 14 Organic Compounds over the 50-2000 Ev Range. *Surf. Interf. Anal.* **1994**, *21*, 165-176.

(22) Chen, Y.; Ding, H.; Sun, S. Preparation and Characterization of ZnO Nanoparticles Supported on Amorphous SiO_2. *Nanomaterials* **2017**, *7*, 217.

(23) Lee, J. H.; Kim, C. H.; Kim, H. S.; Park. J. H.; Ryu, J. H.; Baek, K. H.; Do, L. M. Stability Characteristics of Gallium-Doped Zinc-Tin-Oxide Thin-Film Transistors Fabricated Using a Sol-Gel Method. *J. Korean Phys. Soc.* **2013**, *62*, 1176-1182.

(24) Deng, X.; Verdaguer, A.; Herranz, T.; Weis, C.; Bluhm, H.; Salmeron, M. Surface Chemistry of Cu in the Presence of CO_2 and H_2O. *Langmuir* **2008**, *24*, 9474-9478.

(25) Bluhm, H.; Hävecker, M.; Knop-Gericke, A.; Kleimenov, E.; Schlögl, R. J. Methanol Oxidation on a Copper Catalyst Investigated Using In Situ X-ray Photoelectron Spectroscopy. *Phys. Chem*. B. **2004**, *108*, 14340-14347.

(26) Wu, C. H.; Eren, B.; Bluhm, H.; Salmeron, M. B. Ambient-Pressure X-Ray Photoelectron Spectroscopy Study of Cobalt Foil Model Catalyst under CO, H_2, and Their Mixtures. *ACS Catal*. **2017**, *7*, 1150-1157.

(27) Al-Gaashani, R.; Radiman, S.; Daud, A. R.; Tabet, N.; Al-Douri, Y. S. XPS and Optical Studies of Different Morphologies of ZnO Nanostructures Prepared by Microwave Methods. *Ceram. Int*. **2013**, *39*, 2283-2292.

(28) Prosvirin, I. P.; Bukhtiyarov, A. V.; Bluhm, H.; Bukhtiyarov, V. I. Application of Near Ambient Pressure Gas-Phase X-Ray Photoelectron Spectroscopy to the Investigation of Catalytic Properties of Copper in Methanol Oxidation. *Appl. Surf. Sci.* **2016**, *363*, 303-309.

(29) F.; Owens, A. W.; Rajumon, M. K.; Roberts, M. W.; Jackson, S. D. Oxidation of Methanol at Copper Surfaces. *Catal. Lett.* **1996**, *37*, 79-87.

(30) Zhang, Y.; Savara, A.; Mullins, D. R. Ambient-Pressure XPS Studies of Reactions of Alcohols on $SrTiO_3$ (100). *J. Phys. Chem. C* **2017**, *121*, 23436-23445.

(31) Hadjiivanov, K. I.; Vayssilov, G. N. Characterization of Oxide Surfaces and Zeolites by Carbon Monoxide as an IR Probe Molecule. *Adv. Catal.* **2002**, *47*, 307-511.

(32) Prieto, G.; Martinez, A.; Concepcion, P.; Moreno-Tost, R. Cobalt Particle Size Effects in Fischer–Tropsch Synthesis: Structural and In Situ Spectroscopic Characterisation on Reverse Micelle-Synthesised Co/ITQ-2 Model Catalysts. *J. Catal*. **2009**, *266*, 129-144.

(33) Boronat, M.; Concepcion, P.; Corma, A. Unravelling the Nature of Gold Surface Sites by Combining IR Spectroscopy and DFT Calculations. Implications in Catalysis. *J. Phys. Chem. C* **2009**, *113*, 16772-16784.

- **GRAPHICAL ABSTRACT**